Laser and Particle Beams (2007), *25*, 339–346. Printed in the USA.

DOI: 10.1017/S0263034607000195

Relativistic plasma control for single attosecond pulse generation: Theory, simulations, and structure of the pulse

T. BAEVA,[1] S. GORDIENKO,[2] AND A. PUKHOV[1]

[1]Institut für Theoretische Physik I, Heinrich-Heine-Universität Düsseldorf, Düsseldorf Germany
[2]L.D. Landau Institute for Theoretical Physics, Moscow, Russia

(Received 27 November 2006; Accepted 15 February 2007)

Abstract

The method of relativistic plasma control (RPC) for generation of single (sub-) attosecond pulses based on high harmonic generation at plasma surface is presented. Use is made of the concept of apparent reflection point (ARP), introduced for the sake of analytical treatment of the plasma dynamics. We show theoretically and numerically that managing the laser polarisation the ARP dynamics can be efficiently controlled and a single ultra-short pulse can be extracted out of the short pulse train generated by a multi-cycle driver. For the sake of future applications the structure of the pulse is studied analytically and numerically by particle-in-cell simulations.

Keywords: Attosecond pulses; High harmonics; Relativistic plasma

1. INTRODUCTION

The interaction of strong laser pulses with solids is accompanied by the generation of high order harmonics. This spectacular phenomenon was observed for the first time with nanosecond CO_2 laser light pulses of μm-wavelength (Carman *et al.*, 1981). Shortly after the experimental observation in 1981, the problem of harmonic light emission was studied theoretically (Bezzerides *et al.*, 1982). This approach based on non-relativistic equations of motion and hydrodynamic approximation for the plasma predicted a cutoff of the harmonic spectrum at the plasma frequency.

Roughly 10 years later, in 1993, a new approach to the interaction of an ultra short, relativistically strong laser pulse with overdense plasma was proposed (Bulanov *et al.*, 1993). The authors "interpreted the harmonic generation as due to the Doppler effect produced by a reflecting charge sheet, formed in a narrow region at the plasma boundary, oscillating under the action of the laser pulse" (Bulanov *et al.* 1993). The "oscillating mirror" model predicts a cutoff harmonic number of $4\gamma_{\max}^2$, where $\gamma_{\max}$ is the maximal γ-factor of the mirror.

At the beginning of 1996, numerical results of particle-in-cell simulations of the harmonic generation by femtosecond laser-solid interaction were presented (Gibbon, 1996). In this work, it was demonstrated numerically that the high harmonic spectrum goes well beyond the cutoff predicted in Bezzerides *et al.* (1982) and also presented a numerical fit for the spectrum, which approximated the intensity of the n-th harmonic as $I_n \propto n^{-5}$. At about the same time the laser-overdense plasma interaction was also studied by Lichters *et al.* (1996).

In the same year, the analytical work by von der Linde and Rzazewski appeared. The authors used the "oscillating mirror" model and approximated the oscillatory motion of the mirror as a sin-function of time, without analysis of the applicability of this approximation. With this explicit form of the mirror motion, an analytical formula for the harmonic spectrum was obtained.

The first try to describe analytically the high harmonics generated at the boundary of overdense plasma, by a short ultra intense laser pulse in a universal way, that does not rely on an explicit formula for the exact plasma mirror motion was made in Gordienko *et al.* (2004). This work proposed for the first time the idea of universality of the harmonic spectrum. Making use of the steepest descent method, Gordienko *et al.* (2004) have shown that the harmonic spectrum follows a slowly decaying power law $I_n \propto n^{-p}$, where the exponent p was expected to be $p = 2.5$.

The analytically predicted power law spectrum has found a spectacular independent experimental confirmation in the recently published paper (Dromey *et al.*, 2006). This

Address correspondence and reprint requests to: T. Baeva, Institut für Theoretische Physik I, Heinrich-Heine-Universität Düsseldorf, Universitätsstr. 1, Geb.25.32, 40225 Düsseldorf, Germany. E-mail: tbaeva@tp1.uni-duesseldorf.de

experiment confirms the power law spectrum decay down to the "water window" range, and thus demonstrates that the high harmonics generated at plasma surfaces in the relativistic regime represent a phenomenon of particular interest, not only for its physical nature but, most important, for its various applications. Among these is the generation of short wavelength radiation and attosecond pulses, necessary for the study of ultra-fast processes in atoms, molecules, and solids at intensities significantly higher than those obtained from strong field laser-atom interactions (Kienberger *et al.*, 2004; Itatani *et al.*, 2004; Niikura *et al.*, 2002), as well as for the high contrast study of biological samples (Ozaki *et al.*, 2006; Ozaki *et al.*, 2007).

The plasma harmonics are generated in the relativistic regime, when the laser pulse intensity is $I \gg 10^{18}\,\mathrm{W/cm^2}$. Laser pulses of such intensity usually are several cycles long (Fuerbach *et al.*, 2005). As a consequence, the reflected radiation contains a comb of attosecond pulses. For various applications, e.g., molecular imaging (Itatani *et al.*, 2004; Niikura *et al.*, 2002; Lein *et al.*, 2002), usually a single short pulse is needed to prevent undesirable effects. The single attosecond pulse can be selected using a phase-stabilized single cycle laser (Kienberger *et al.*, 2004). An elegant way to control the atomic response by time-dependent laser polarization has been proposed earlier in the context of gas harmonics (Ivanov *et al.*, 1995).

In this work, we show that managing the polarization of the incident laser pulse allows to extract a single (sub-) attosecond pulse from relativistically driven plasma surface in a well controlled way. Physically, the control is performed over the relativistic γ-factor of the apparent reflection point (ARP) (Baeva *et al.*, 2006*a*, 2006*b*). Although the driving laser pulse can be long and intense, the ARP velocity becomes highly relativistic only at the specific time, when the vector potential component tangential to the plasma surface vanishes, and at this moment, the single attosecond pulse is emitted. A pulse with time-dependent polarization can be equivalently represented as a superposition of two perpendicularly polarized laser pulses with slightly different frequencies and a phase shift (see Fig. 1). Experimentally, the time-dependent laser pulse ellipticity can be achieved by femtosecond polarization pulse shaping techniques (Brixner *et al.*, 2004).

We also study the structure of the attosecond pulses generated after filtering of the high harmonic radiation at relativistic plasma surfaces depending on the filter position.

2. APPARENT REFLECTION POINT

Consider the interaction of a short ultra-intense laser pulse with a slab of overdense plasma. During the short interaction time, we can neglect the ion motion and study the electron fluid oscillations only. It was shown in Gordienko *et al.* (2004) that to describe the high harmonic generation

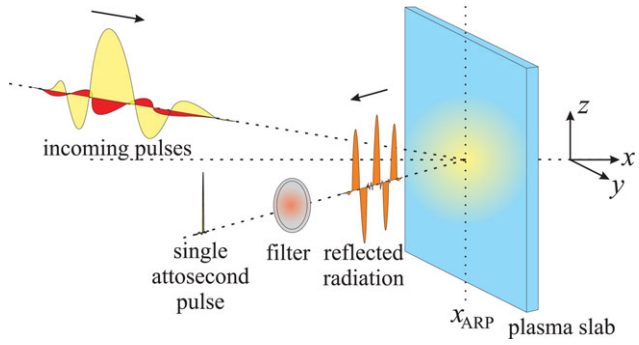

Fig. 1. Geometry for relativistic plasma control of attosecond plasma surface dynamics. The polarization of the high intensity driving pulse is managed by a low intensity controlling pulse. After proper filtering of the reflected radiation, a single attosecond pulse can be isolated. The interaction process can be described in terms of the ARP. It appears to an external observer that the radiation electric field is zero at the ARP.

analytically, the boundary condition

$$\mathbf{E}_\tau = 0 \tag{1}$$

must be used. Here $\mathbf{E}_\tau$ is the tangential to the plasma surface component of a constructed electric field, which coincides with the physical electric field outside the plasma, and satisfies the vacuum wave equation everywhere. The electric field constructed this way differs from the real electric field inside the plasma slab. Yet, this construction is sufficient to get all of the information about the high harmonic spectrum (Baeva *et al.*, 2006*a*).

The boundary condition (1) stated for the constructed field is exact, what would not be the case for the physical electric field (Baeva *et al.*, 2006*b*).

The boundary condition (1) allows to describe analytically the ARP. We represent the electric field as the sum of the incident and the reflected radiation. The incident laser field in vacuum runs in the positive x-direction, $\mathbf{E}^{\mathrm{i}}(x,t) = \mathbf{E}^{\mathrm{i}}(x - ct)$, while the reflected field is translated backward: $E^r(x,t) = \mathbf{E}^r(x + ct)$. The tangential components of these fields interfere destructively at the ARP position $x_{\mathrm{ARP}}(t)$, so that the implicit equation for the apparent reflection point $x_{\mathrm{ARP}}(t)$ is:

$$\mathbf{E}^{\mathrm{i}}_\tau(x_{\mathrm{ARP}} - ct) + \mathbf{E}^r_\tau(x_{\mathrm{ARP}} + ct) = 0. \tag{2}$$

We point out again that Eq. (2) contains the electromagnetic fields in vacuum. That is why the reflection point x_{ARP} is apparent. The real interaction within the plasma skin layer can be very complex. Yet an external observer who has information about the radiation in vacuum only, sees that $\mathbf{E}_\tau$ vanishes at x_{ARP}. The ARP is located within the skin layer at the electron fluid surface, which is much shorter than the laser wavelength for overdense plasmas.

https://doi.org/10.1017/S0263034607000195 Published online by Cambridge University Press

3. RESULTS FROM ULTRA-RELATIVISTIC SIMILARITY THEORY

The ARP dynamics completely defines the high harmonic generation. In the ultra-relativistic regime, when the dimensionless vector potential $a_0 = eA_0/mc^2$ of the laser is large, $a_0^2 \gg 1$, we can apply ultra-relativistic similarity theory (Gordienko & Pukhov, 2005) to characterize this motion. Basically this theory states that when we change the plasma density N_e and the laser amplitude a_0 simultaneously keeping constant the similarity parameter defined by

$$S = N_e/a_0 N_c = \text{const}, \tag{3}$$

the laser-plasma dynamics remains similar. Here $N_c = \omega_0^2\, m/4\pi e^2$ is the critical plasma density for the laser pulse with the frequency ω_0. This means that for different interactions with the same similarity parameter $S = \text{const}$, the plasma electrons move along the same trajectories, while their momenta $\mathbf{p}$ scale with the laser amplitude: $\mathbf{p} \propto a_0$. Consequently, the electron momentum components tangential and normal to the plasma surface scale simultaneously with a_0:

$$\mathbf{p}_\tau \propto a_0; \quad \mathbf{p}_n \propto a_0. \tag{4}$$

Therefore, in general, the total electron momenta are not perpendicular to the surface. Moreover, the characteristic angle between their direction and the surface normal does not depend on a_0 provided that S is fixed.

This result is crucial for the plasma surface dynamics. Since we consider an ultra-relativistic laser pulse with $a_0^2 \gg 1$, the electrons in the skin layer move with ultra-relativistic velocities almost all the time:

$$v = c\sqrt{\frac{\mathbf{p}_n^2 + \mathbf{p}_\tau^2}{m_e^2c^2 + \mathbf{p}_n^2 + \mathbf{p}_\tau^2}} = c[1 - O(a_0^{-2})]. \tag{5}$$

Yet the relativistic γ-factor of the plasma surface $\gamma_s(t)$ and its velocity $v_s(t)$ behave in a quite different way. Let us consider electrons at the very boundary of the plasma. The similarity theory states that the electron momenta can be represented as

$$\begin{aligned} \mathbf{p}_n(t) &= a_0 \mathbf{P}_n(S, \omega t), \\ \mathbf{p}_\tau(t) &= a_0 \mathbf{P}_\tau(S, \omega t), \end{aligned} \tag{6}$$

where $\mathbf{P}_n$ and $\mathbf{P}_\tau$ are universal functions, which do not depend on a_0 explicitly, but rather on the similarity parameter S, and on the pulse shape. Thus, the plasma surface velocity $\beta_s(t) = v_s(t)/c$ and $\gamma_s(t)$ are

$$\begin{aligned} \beta_s(t) &= \frac{p_n(t)}{\sqrt{m_e^2c^2 + \mathbf{p}_n^2(t) + \mathbf{p}_\tau^2(t)}}, \\ &= \frac{P_n(t)}{\sqrt{\mathbf{P}_n^2(t) + \mathbf{P}_\tau^2(t)}} - O(a_0^{-2}), \end{aligned} \tag{7}$$

$$\gamma_s(t) = \frac{1}{\sqrt{1 - \beta_s^2(t)}} = \sqrt{1 + \frac{\mathbf{P}_n^2(t)}{\mathbf{P}_\tau^2(t)}} + O(a_0^{-2}). \tag{8}$$

It follows from Eqs. (7)–(8) that the relativistic γ-factor of the plasma boundary is of the order of unity for almost all times, except for those times t_g, when the tangential momentum component vanishes:

$$\mathbf{p}_\tau(S, t_g) = 0, \tag{9}$$

Exactly at these times, there are spikes of the γ-factor:

$$\gamma_s = \frac{1}{\sqrt{1 - \beta_s^2}} = \sqrt{\frac{\mathbf{p}_n^2 + m_e^2c^2}{m_e^2c^2}} \propto a_0. \tag{10}$$

On the contrary, the plasma surface velocity v_s as given by Eq. (7), is a smooth function with well defined maxima. It approaches $\pm c$ when the electron momentum parallel to the surface vanishes, i.e., at the same times t_g corresponding to the γ-spikes. The high harmonics are generated at the spikes, when the surface velocity is negative and close to $-c$.

4. RELATIVISTIC PLASMA CONTROL (RPC)

As previously mentioned, it is of great importance to have a single short pulse, instead of a train of short pulses. We have shown above that the attosecond pulses are emitted when the tangential components of the surface electron momentum vanish. This property can be used to control the high harmonic generation and to extract a particular attosecond pulse out of the train.

In the one-dimensional geometry, the transverse generalized momentum is conserved: $\mathbf{p}_\tau = e\mathbf{A}_\tau/c$, where $\mathbf{p}_\tau$ and $\mathbf{A}_\tau$ are the tangential components of the electron momentum $\mathbf{p}$ and the vector potential $\mathbf{A}$. Consequently, the attosecond pulses are emitted when the vector potential is zero. If the vector potential vanishes at several moments, there are several γ-spikes and correspondingly, after proper filtering, several short pulses are observed in the reflected radiation, (see Fig. 3b).

To select a single attosecond pulse, we must ensure that the vector potential $\mathbf{A}_\tau$ turns zero exactly once. Since $\mathbf{A}_\tau$ has two components, how often it vanishes depends on its polarization. For linear polarization, it vanishes twice per laser period, while for circular or elliptic polarization, it never equals zero. A laser pulse with a time-dependent polarization

https://doi.org/10.1017/S0263034607000195 Published online by Cambridge University Press

can be prepared in such a way that its vector potential circles around the zero axis and touches it exactly once.

5. SPIKE DURATION VS. ATTOSECOND PULSE DURATION

It is possible to estimate the width of a γ-spike. Since the surface velocity is a smooth function, we can expand it in Taylor series around the maximum as

$$v_s(t) \approx v_{max} - \alpha\omega_0^2(t - t_{max})^2, \tag{11}$$

where the parameter α depends only on S. The width $\Delta t = |t - t_{max}|$ of the γ_s spikes is then

$$\Delta t \propto \sqrt{1 - v_{max}^2/c^2}/(\omega_0\sqrt{\alpha}) = 1/(\omega_0\sqrt{\alpha}\gamma_{max}). \tag{12}$$

It follows from Eq. (12) that the γ_s spikes get higher and narrower when we increase a_0, keeping $S = \text{const}$. The (sub-) attosecond pulses (Gordienko *et al.*, 2004) are emitted exactly at the times of the spikes, which enables us to find a scaling for the attosecond pulse duration. Since the plasma moves together with the high energy photons, the attosecond pulse duration τ_x is shorter than the γ-spike duration:

$$\tau_x \propto (1 - \beta_s)\Delta t \propto 1/(\omega_0\sqrt{\alpha}\gamma_s^3). \tag{13}$$

Of course, to observe the short attosecond pulse, one has to filter out the lower harmonics in the spectrum, and the actual pulse duration depends on the lower filter cut-off. Though the duration of the shortest pulse which can be obtained scales as

$$\tau_x \propto 1/(\omega_0\gamma_{\max}^3). \tag{14}$$

The physical origin of this favorable $\gamma_{\max}^{-3}$ scaling of the pulse duration is provided by the γ-spikes in the plasma surface dynamics.

6. STRUCTURE OF THE FILTERED PULSE

It is clear that the structure of the filtered pulse will depend on the way of filtration, in particular on the position of the filter. We want to study analytically the process of filtration in order to obtain quantitative characteristics of the pulse structure. The reflected from the plasma surface radiation can be expressed as follows. For the intensity of the nth harmonic we have (Baeva *et al.*, 2006*a*)

$$I_n \propto |\exp(i\Theta_+(n))F(n) - \exp(i\Theta_-(n))F(-n)|^2, \tag{15}$$

where

$$F(n) = \frac{4\sqrt{\pi}}{(\sqrt[4]{\alpha}n)^{4/3}} Ai\left(\frac{2n - n_{cr}}{n_{cr}(\alpha n)^{1/3}}\right), \tag{16}$$

$$\Theta_\pm(n) = \pm\Theta_0 - n\Theta_1. \tag{17}$$

Here $Ai(x)$ denotes the Airy function and n_{cr} denotes the critical harmonic number satisfying $n_{cr} = 4\gamma_{\max}^2$, where $\gamma_{\max}$ is the largest relativistic factor of the plasma boundary. Θ_1 is the time of observation, and Θ_0 is the phase of the incident laser pulse at the time of the γ-spike. Using the representations of the Airy function, one can obtain explicitly the well known universal law for the high harmonic spectrum decay. For $n < \sqrt{\alpha}/8\, n_{cr}^{3/2}$ $(2|1 - n/n_{cr}| \ll (\alpha n)^{1/3})$

$$I_n \propto 1/n^{8/3}; \tag{18}$$

and for $n > \sqrt{\alpha}/8 n_{cr}^{3/2}$ $(2|1 - n/n_{cr}| \gg (\alpha n)^{1/3})$

$$I_n \propto \frac{n_{cr}^{1/2}}{n^3}\exp\left(-\frac{16\sqrt{2}}{3\alpha^{1/2}}\frac{n - n_{cr}}{n_{cr}^{3/2}}\right). \tag{19}$$

Let us apply to this radiation a high-frequency filter that suppresses all harmonics with frequencies below Ω_f, and study how the relative position of the Ω_f and the spectrum cutoff affects the duration of the resulting (sub-)attosecond pulses.

The electric field of the pulse after the filtration is

$$E \propto Re\int_{\Omega_f/\omega_0}^{+\infty} [\exp(i\Theta_+(n)(F(n) - \exp(i\Theta_-(n))F(-n)] \times \exp(int)\, dn. \tag{20}$$

The structure of the filtered pulses depends on where we set the filter threshold Ω_f. In the case $1 \ll \Omega_f/\omega_0 \ll \sqrt{\alpha}/8\, n_{cr}^{3/2}$, we use Eq. (18) and rewrite Eq. (20) as

$$E \propto Re\int_{\Omega_f/\omega_0}^{+\infty} \frac{\exp(int)}{n^{4/3}}\, dn = \left(\frac{\omega_0}{\Omega_f}\right)^{1/3} Re\exp(i\Omega_f t - i\Theta_1)P(\Omega_f t), \tag{21}$$

where the function P

$$P(x) = \int_1^{+\infty} \frac{\exp(iyx)}{y^{4/3}}\, dy \tag{22}$$

gives the slow envelope of the pulse.

It follows from Eq. (21) that the electric field of the filtered pulse decreases very slowly with the filter threshold as $\Omega_f^{-1/3}$. The pulse duration decreases as $1/\Omega_f$. At the same time, the fundamental frequency of the pulse is Ω_f. Therefore the pulse is hollow when $\Omega_f/\omega_0 \ll \sqrt{8\alpha}\gamma_{\max}^3$,

https://doi.org/10.1017/S0263034607000195 Published online by Cambridge University Press

i.e., its envelope is not filled with electric field oscillations. One possible application of these pulses is to study atom excitation by means of a single strong kick.

The pulses structure changes significantly when the filter threshold is placed above the spectrum cutoff. For $\Omega_f/\omega_0 \gg \sqrt{8\alpha\gamma_{\max}^3}$ we use Eqs. (19) and (20) to obtain

$$E \propto \left(\frac{\omega_0}{\Omega_f}\right)^{3/2} \exp\left(-\frac{8\sqrt{2}\Omega_f}{3\sqrt{\alpha}\omega_0 n_{cr}^{3/2}}\right) Re \frac{\exp\left(i\Omega_f t - i\Theta_1\right)}{8\sqrt{2}/\left(3\sqrt{\alpha}n_{cr}^{3/2}\right) + i\omega_0 t}. \tag{23}$$

The amplitude of these pulses decreases fast when Ω_f grows. However, the pulse duration $\propto 1/\sqrt{\alpha\gamma_{\max}^3}$ does not depend on Ω_f. Since the fundamental frequency of the pulse grows as Ω_f, the pulses obtained with an above-cutoff filter are filled with electric field oscillations.

7. NUMERICAL RESULTS

The analytical results presented above can be checked numerically. For this we study the motion of the plasma boundary and the specific behavior of v_{ARP} and γ_{ARP}, as well as the high harmonic radiation and the dependence of the filtered pulses on the position of the filter, using the one-dimensional particle-in-cell code virtual laser-plasma lab (Pukhov, 1999). The plasma slab is initially positioned between $x_L = 1.5\lambda$ and $x_R = 3.9\lambda$, where $\lambda = 2\pi/\omega_0$ is the laser wavelength. The laser pulse is represented by a gaussian envelope of width $\sigma = 2\lambda$:

$$a(x, t = 0) = a_0 \exp\left(-x^2/\sigma^2\right) \cos\left(2\pi x/\lambda\right). \tag{24}$$

An external observer positioned at $x = 0$ records the incident and the reflected fields at every time step. This observer can easily chase these fields to arbitrary x and t since these fields are solutions of the wave equation in vacuum. To find the ARP position x_{ARP}, we solve numerically Eq. (2). The trajectory of $x_{\mathrm{ARP}}(t)$ for the simulation parameters $a_0 = 20$ and $N_e/N_c = 90$ $(S = 4.5)$ is presented in Figure 2a. One can clearly see the oscillatory motion of the point $x_{\mathrm{ARP}}(t)$. The equilibrium position is displaced from the initial plasma boundary position x_L due to the mean laser light pressure.

Since only the ARP motion toward the laser pulse is of importance for the high harmonic generation, we cut out the positive ARP velocities $v_{\mathrm{ARP}}(t) = dx_{\mathrm{ARP}}(t)/dt$ and calculate only the negative ones, Figure 2b, because in our geometry, negative velocity corresponds to motion toward the laser pulse. The corresponding γ-factor

$$\gamma_{\mathrm{ARP}}(t) = 1/\sqrt{1 - v_{\mathrm{ARP}}(t)^2/c^2} \tag{25}$$

is presented in Figure 2c. Notice that the ARP velocity is a smooth function around its maxima, resembling a parabola rather than a flat plateau. At the same time, the γ-factor $\gamma_{\mathrm{ARP}}(t)$ contains sharp spikes, which coincide with the velocity extrema. These spikes of the surface γ-factor are responsible for the high harmonic generation.

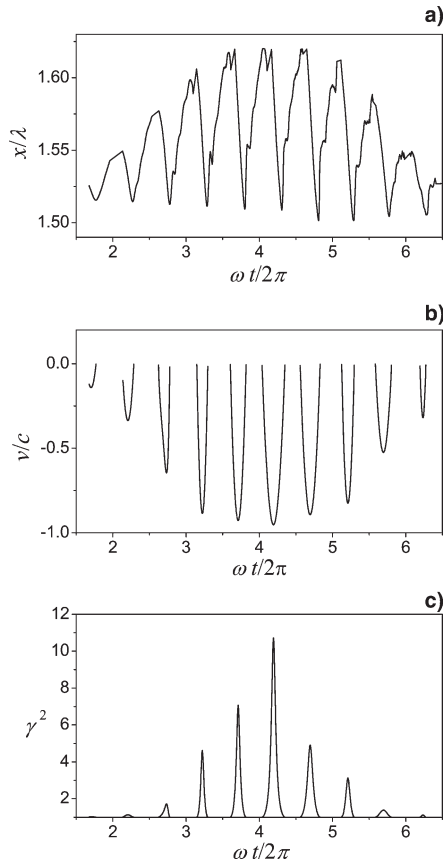

Fig. 2. One-dimensional particle-in-cell simulation results for the parameters $a_0 = 20$ and $N_e = 90\,N_c$. (**a**) Oscillatory motion of the point $x_{\mathrm{ARP}}(t)$ where $\mathbf{E}_\tau(x(t)) = 0$. (**b**) Velocity $v_{\mathrm{ARP}}(t) = dx_{\mathrm{ARP}}(t)/dt$; only the negative velocities are shown. Notice that the ARP velocity is a smooth function around its maxima. (**c**) The corresponding γ-factor $\gamma_{\mathrm{ARP}}(t) = 1/\sqrt{1 - v_{\mathrm{ARP}}(t)^2/c^2}$ contains sharp spikes, which coincide with the velocity extrema.

The numerically obtained spectrum of the high-harmonics is shown in Figure 3a. Filtering out the lower harmonics and keeping only the harmonics with $\omega > 25\omega_0$, we obtain a train of short pulses in the reflected radiation, Figure 3b.

In order to simulate numerically the technique of RPC for generation of a single (sub-) attosecond pulse, we study the interaction of the plasma with a laser pulse of time-dependent polarization. This pulse can be equivalently represented as a superposition of two perpendicularly polarized laser pulses with slightly different frequencies, (see Fig. 1). Our particle-in-cell simulations suggest that a signal with a few percent of the driver intensity is sufficient to control the high harmonic generation, if the phase difference between the two laser pulses is chosen carefully.

To demonstrate the relativistic plasma control, we perform a particle-in-cell simulation where we add the z-polarized controlling pulse with amplitude $a_c = 6$ and frequency

https://doi.org/10.1017/S0263034607000195 Published online by Cambridge University Press

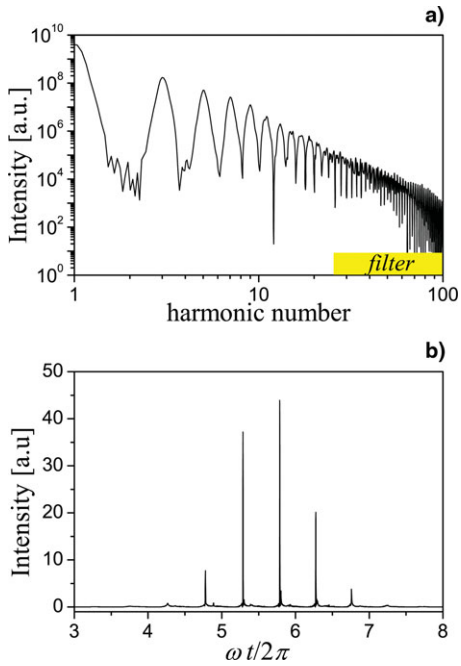

Fig. 3. (**a**) The high harmonics spectrum; (**b**) the train of attosecond pulses is obtained after the proper filtering.

$\omega_c = 1.25$, and retain the same driver pulse with amplitude $a_0 = 20$, frequency $\omega_0 = 1$, and y-polarization. We keep the same plasma density $N_e/N_c = 90$. The optimal phase difference between the two lasers is found empirically to be $\Delta\phi = \pi/8$. The vector potential of the resulting laser pulse is represented as a function of time in Figure 4.

The simulation results are presented in Figures 5a and 5b. Comparing the surface γ-factor dynamics in the regime of linear polarization, Figure 2c and in the controlled regime, Figure 5a, we see that the central γ-spike is slightly larger while both side spikes are significantly damped. This effect becomes much more pronounced when we compare the filtered radiation plots, Figure 3b and Figure 5b. The control

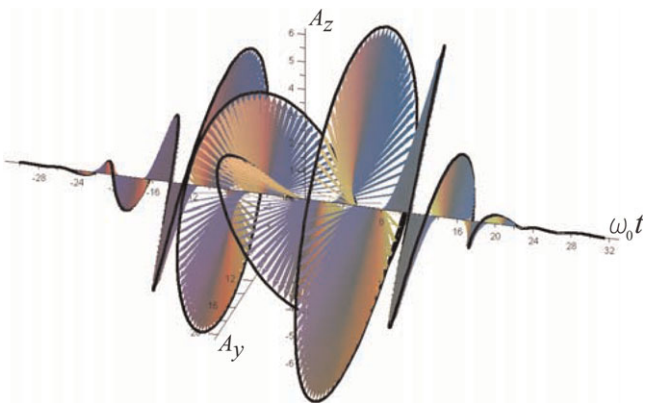

Fig. 4. Vector potential of the polarization-managed laser pulse: driver pulse with amplitude $a_0 = 20$, frequency $\omega_0 = 1$ and y-polarization; z-polarized controlling pulse with amplitude $a_c = 6$ and frequency $\omega_c = 1.25$; phase shift $\Delta\phi = \pi 8$.

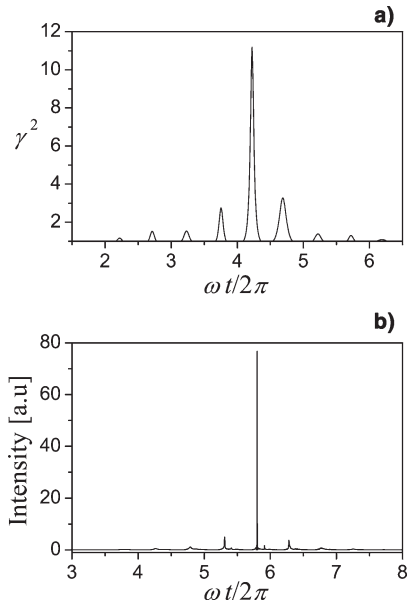

Fig. 5. Generation of a single attosecond pulse using the relativistic plasma control. The driver signal has $a_0 = 20$ and frequency $\omega_0 = 1$. The controlling signal has $a_c = 6$ and frequency $\omega_c = 1.25$. The phase difference is $\Delta\phi = \pi/8$. (**a**) the γ-spikes of the oscillating ARP, (**b**) the single attosecond pulse selected via the relativistic plasma control.

signal allows us to select the single attosecond pulse corresponding to the highest γ-spike in the surface motion.

Varying the control parameters a_0/a_c, ω_0/ω_c and $\Delta\phi$ we are able to select different attosecond pulses one-by-one or in groups out of the original pulse train.

The dependence of the short pulses on the position of the filter also can be studied numerically. If we apply the filter $f(\omega) = 1 + \tanh((\omega\text{-}\Omega_f)/\Delta\omega)$, frequencies below Ω_f are suppressed. We choose the simulation case of laser vector potential $a_0 = 20$ and plasma density $N_e = 90\ N_c$. The spectrum of high harmonics is given in Figure 3. We zoom in to one of the pulses in the pulse train obtained and study how the shape of this one pulse changes with Ω_f. Figure 6 represents the pulse behavior for four different positions of Ω_f. We measure to what degree the pulse is filled by the number of field oscillations within the full width at half maximum. One clearly sees that for filter threshold below $\omega_0\sqrt{8\alpha\gamma_{max}^3}$ frequency, Figures 6a, 6b, the pulse is hollow. Notice that the case of Figure 6b corresponds to the cutoff frequency predicted by the "oscillating mirror" model. Only for filter threshold positions above $\omega_0\sqrt{8\alpha\gamma_{max}^3}$ the pulse becomes filled, Figures 6c, 6d, in agreement with the theoretical prediciton presented in Section 6.

8. CONCLUSIONS

To recapitulate, we studied analytically and numerically the dynamics of the apparent reflection point at the surface of overdense plasma. We have shown that the velocity of this point is a smooth function of time. However, the corresponding γ-factor has quasi-singularities or spikes when the

https://doi.org/10.1017/S0263034607000195 Published online by Cambridge University Press

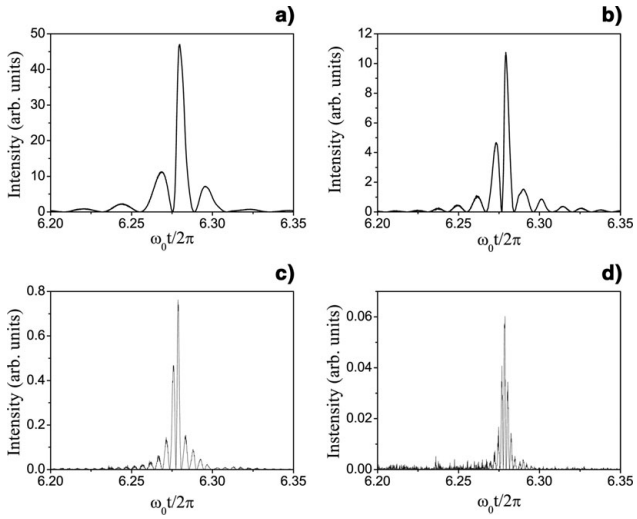

Fig. 6. Dependence of the pulses filling on the position of the sharp filter boundary for $a_0 = 20$ and $N_e = 90\,N_c$ and filter positions: (**a**) $\Omega_f = 20\omega_0$, $\Delta\omega = 2\omega_0$; (**b**) $\Omega_f = 40\omega_0$, $\Delta\omega = 2\omega_0$; (**c**) $\Omega_f = 100\omega_0$, $\Delta\omega = 2\omega_0$; (**d**) $\Omega_f = 200\omega_0$, $\Delta\omega = 2\omega_0$.

surface velocity approaches the speed of light. These ultrarelativistic spikes are responsible for the high harmonic generation in the form of an attosecond pulse train. We show that the attosecond pulse emission can be efficiently controlled by managing the laser polarization. This is done by adding a low intensity controlling pulse with perpendicular polarization and frequency slightly different from that of the driving pulse. This relativistic plasma control allows to extract a single attosecond pulse or a prescribed group of attosecond pulses. The attosecond pulses generated at plasma surfaces can be filled with oscillations or empty, depending on the position of the filter.

ACKNOWLEDGMENTS

This work has been supported in parts by DFG Transregio 18 and by DFG Graduierten Kolleg 1203.

REFERENCES

Baeva, T., Gordienko, S. & Pukhov, A. (2006*a*). Theory of high-order harmonic generation in relativistic laser interaction with overdense plasma. *Phys. Rev. E* **74**, 046404.

Baeva, T., Gordienko, S. & Pukhov, A. (2006*b*). Relativistic plasma control for single attosecond X-ray burst generation. *Phys. Rev. E* **74**, 065401.

Bezzerides, B., Jones, R.D. & Forslund, D.W. (1982). Plasma mechanism for ultraviolet harmonics radiation due to intense CO_2 light. *Phys. Rev. Lett.* **49**, 202.

Brixner, T., Krampert, G., Pfeifer, T., Selle, R., Gerber, G., Wollenhaupt, M., Graefe, O., Horn, C., Liese, D. & Baumert, T. (2004). Quantum control by ultrafast polarization shaping. *Phys. Rev. Lett.* **92**, 208301.

Bulanov, S.V., Naumova, N.M. & Pegoraro, F. (1993). Interaction of an ultrashort, relativistically strong laser pulse with an overdense plasma. *Phys. Plasmas* **1**, 745.

Carman, R.L., Forslund, D.W. & Kindel, J.M. (1981). Visible harmonic emission as a way of measuring profile steepening. *Phys. Rev. Lett.* **46**, 29.

Dromey, B., Zepf, M., Gopal, A., Lancaster, K., Wei, M.S., Krushelnick, K., Tatarakis, M., Vakakis, N., Moustaizis, S., Kodama, R., Tampo, M., Stoeckl, C., Clarke, R., Habara, H., Neely, D., Karsch, S. & Norreys, P. (2006). High harmonic generation in the relativistic limit. *Nature Phys.* **2**, 456–459.

Fuerbach, A., Fernandez, A., Apolonski, A., Fuji, T. & Krausz, F. (2005). Chirped-pulse oscillators for the generation of high-energy femtosecond laser pulses. *Laser Part. Beams* **23**, 113–116.

Gibbon, P. (1996). Harmonic generation by femtosecond laser-solid interaction: a coherent "water-window" light source? *Phys. Rev. Lett.* **76**, 50.

Gordienko, S., Pukhov, A., Shorokhov, O. & Baeva, T. (2004). Relativistic doppler effect: Universal spectra and zeptosecond pulses. *Phys. Rev. Lett.* **93**, 115002.

Gordienko, S. & Pukhov, A. (2005). Scalings for ultrarelativistic laser plasmas and quasimonoenergetic electrons. *Phys. Plasmas* **12**, 043109.

Itatani, J., Levesque, J., Zeidler, D., Niikura, H., Papin, H., Kieffer, J.C., Corkum, P.B. & Villeneuve, D.M. (2004). Tomographic imaging of molecular orbitals. *Nature* **432**, 867–871.

Ivanov, M., Corkum, P.B., Zuo, T. & Bandrauk, A. (1995). Routes to control of intense-field atomic polarizability. *Phys. Rev. Lett.* **74**, 2933–2936.

Kienberger, R., Goulielmakis, E., Uiberacker, M., Baltuska, A., Yakovlev, V., Bammer, F., Scrinzi, A., Westerwalbesloh, Th., Kleineberg, U., Heinzmann, U., Drescher, M. & Krausz, F. (2004). Atomic transient recorder. *Nature* **427**, 817–821.

Lein, M., Hay, N., Velotta, R., Marangos, J.P. & Knight, P.L. (2002). Interference effects in high-order harmonic generation with molecules. *Phys. Rev. A* **66**, 023805.

Lichters, R., Meyer-ter-Vehn, J. & Pukhov, A. (1996). Short-pulse laser harmonics from oscillating plasma surfaces driven at relativistic intensity. *Phys. Plasmas* **3**, 3425–3437.

von der Linde, D., Engers, T., Jenke, G., Agostini, P., Grillon, G., Nibbering, E., Mysyrowicz, A. & Antonetti, A. (1995). Generation of high-order harmonics from solid surfaces by intense femtosecond laser pulses. *Phys. Rev. A* **52**, R25–R27.

von der Linde, D. & Rzazevski, K. (1996). High-order optical harmonic generation from solid surfaces. *Appl. Phys. B* **63**, 499–506.

Niikura, H., Lagara, F., Hasbani, R., Bandrauk, A.D., Ivanov, M., Villeneuve, D.M. & Corkum, P.B. (2002). Sub-laser-cycle electron pulses for probing molecular dynamics. *Nature* **417**, 917–922.

Norreys, P.A., Zepf, M., Moustaizis, S., Fews, A.P., Zhang, J., Lee, P., Bakarezos, M., Danson, C.N., Dyson, A., Gibbon, P., Loukakos, P., Neely, D., Walsh, F.N., Wark, J.S. & Dangor, A.E. (1996). Efficient extreme UV harmonics generated from picosecond laser pulse interactions with solid targets. *Phys. Rev. Lett.* **76**, 1832–1835.

Ozaki, T., Kieffer, J.C., Toth, R., Fourmaux, S., Bandulet, H. (2006). Experimental prospects at the Canadian advanced laser light source facility. *Laser Part. Beams* **24**, 101–106.

Ozaki, T., Bom, L.B.E., Ganeev, R. & Kieffer, J.C. (2007). Intense harmonic generation from silver ablation. *Laser Part. Beams* **25**, (In press).

Pukhov, A. (1999). Three-dimensional electromagnetic relativistic particle-in-cell code VLPL (Virtual Laser Plasma Lab). *J. Plasma Phys.* **61**, 425–433.

Tsakiris, G., Eidmann, K., Meyer-ter-Vehn, J. & Krausz, F. (2006). Route to intense single attosecond pulses. *New J. Phys.* **8**, 19.

Zepf, M., Tsakiris, G.D., Pretzler, G., Watts, I., Chambers, D.M., Norreys, P.A., Andiel, U., Dangor, A.E., Eidmann, K., Gahn, C., Machacek, A., Wark, J.S. & Witte, K. (1998). Role of the plasma scale length in the harmonic generation from solid targets. *Phys. Rev. E* **58**, R5253–R5256.

https://doi.org/10.1017/S0263034607000195 Published online by Cambridge University Press